Mon. Not. R. Astron. Soc. **000**, 1–11 (2011) Printed 25 February 2013 (MN LaTeX style file v2.2)

arXiv:1203.1452v1 [astro-ph.SR] 7 Mar 2012

Chemical composition of giants from two moving groups

F. Liu,[1,2] Y. Q. Chen,[1] G. Zhao,[1*] I. Han,[3] B. C. Lee,[3] K. M. Kim,[3] Z. S. Zhao[4,5]
[1] *National Astronomical Observatories, Chinese Academy of Sciences, A20, Datun Road, Chaoyang District, Beijing 100012, China*
[2] *Graduate University of the Chinese Academy of Sciences, 19A Yuquan Road, Shijingshan District, Beijing 100049, China*
[3] *Korea Astronomy and Space Science Institute, 61-1, Whaam-dong, Yuseong-gu, Daejeon 305-348, Korea*
[4] *National Astronomical Observatory of Japan, 2-21-1, Osawa, Mitaka, Tokyo 181-8588, Japan*
[5] *The Graduate University for Advanced Studies, Shonan Village, Hayama, Kanagawa 240-0193 Japan*

Accepted 2012 February 20. Received 2012 February 3; in original form 2011 December 20

ABSTRACT

We present stellar parameters of 19 K-type giants and their abundances of 13 chemical elements (Al, Ba, Ca, Fe, K, Mg, Mn, Na, Ni, Sc, Si, Ti and V), selected from two moving groups, covering the metallicity range of -0.6 < [Fe/H] < 0.2, based on high resolution spectra. Most elemental abundances show similar trends with previous studies except for Al, Na and Ba, which are affected by evolution seriously. The abundance ratios of [Na/Mg] increase smoothly with higher [Mg/H] and [Al/Mg] decrease slightly with increasing [Mg/H]. [Mg/Ba] show distinction between these two moving groups which is mainly induced by chemical evolution and partly by kinematic effects. The inhomogeneous metallicity of each star from the moving groups demonstrate that these stars have different chemical origins before they were kinematically aggregated and favor the dynamical resonant theory.

Key words: stars: abundances – stars: fundamental parameters – Galaxy: evolution – open clusters and associations: individual: moving group 6, moving group 7.

1 INTRODUCTION

Research on moving groups can be traced back into a century ago, Proctor (1869) discovered two clearest moving groups in the solar neighborhood (Hyades and Ursa Major), which were the only ones known near Earth for nearly 100 years. Since data of the Hipparcors Satellite (ESA 1997) which consist of accurate parallaxes and proper motions were available, the study of moving groups in the solar vicinity has made great progress. Productive moving groups were identified by their coherent kinematic structures like Pleiades, Ursa, Hyades, Hercules, IC2391, Coma, HR1614 Moving group and so on (Chen et al. 1997; Dehnen 1998; Famaey et al. 2005, 2008; De Silva et al. 2007; Antoja et al. 2008; Klement et al. 2008). Recent work by Zhao et al. (2009) identified 22 moving group candidates with the newly-developed wavelet transform technique by Skuljan et al. (1999). Although these statistical studies of large samples of stars have confirmed the existence of moving groups, their origins and evolution still remain unclear.

According to Eggen (1996), moving groups are the midstep between stars in open clusters and field stars. As open clusters are disrupted by the gravitational effects, their associations stretch into a tube-like structure around the Galactic plane and dissolve into the background after several Galactic orbits. This hypothesis that moving groups are a result of the dispersion of stellar clusters was restricted to young groups of stars with ages less than 1 Gyr, as disk heating and differential Galactic rotation would have dissolved older groups among the field stars. Another theoretical hypothesis in favour of different dynamical origins of moving groups were put forward by Mayor (1972) and Kalnajs (1991). Dehnen (1998) pointed out that most moving groups observed in the solar vicinity could be formed by orbital resonances, related to the Galactic spiral structure, combined with initial velocities of the stars (Skuljan et al. 1999). The works by Famaey et al. (2005, 2007) observed a very wide range of ages for each of kinematic structures in their H-R diagram and found that the Hyades moving group is mixed by stars evaporated from the Hyades cluster and a group of older stars trapped at a resonance. Those minor kinematic groups are related to the accretion events in the Galaxy (Helmi et al. 2006). Nowadays, the second hypothesis with resonant mechanism is considered to be the most plausible explanation for most moving groups (Antoja et al. 2008).

It is crucial to investigate the chemical composition of stars from the moving groups to better understand the origins and evolutionary histories of these groups and give rise to new clues and theories of such kinematic structures. There

---

* E-mail: gzhao@bao.ac.cn

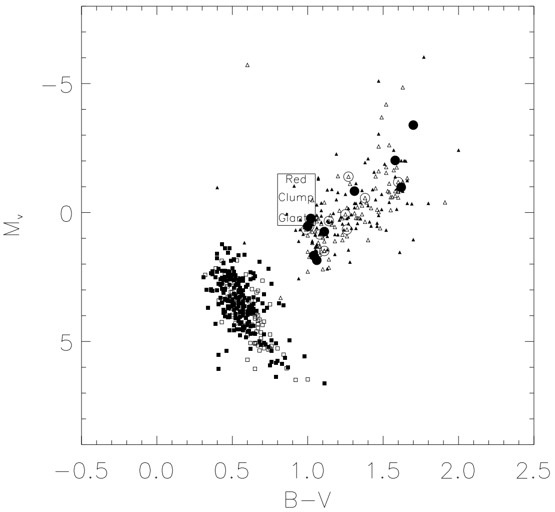

Figure 1. Color magnitude diagram of our sample. Filled rectangles: dwarfs of moving group 6, open rectangles: dwarfs of moving group 7, filled triangles: giants of moving group 6, open triangles: giants of moving group 7, filled circles: our sample stars of moving group 6, open circles: our sample stars of moving group 7.

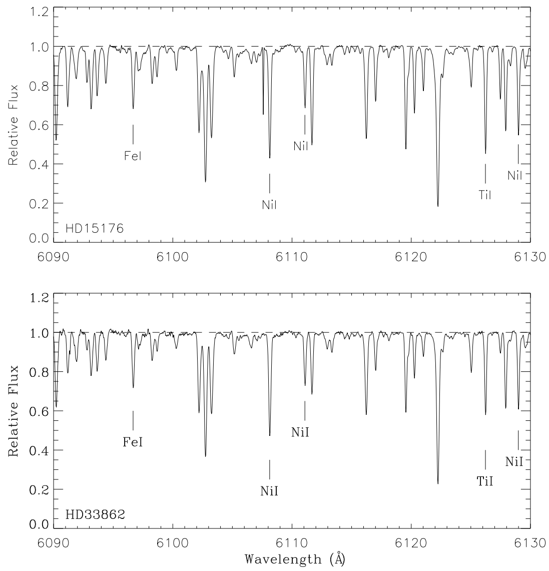

Figure 2. Examples of spectra obtained with BOES at BOAO for HD15176 (T_{eff} = 4556 K, log g = 2.44, [Fe/H] = -0.09) and HD33862 (T_{eff} = 4776 K, log g = 2.60, [Fe/H] = -0.25) with SNR ∼ 180.

have been only a few works analyzing abundances other than iron of moving group stars with high resolution spectra in recent years. This paper focuses on the discussion of 13 elemental abundances of 19 K-type giants from moving group 6 and 7, identified by Zhao et al. (2009), which have opposite U-velocity. We analyze the discrepancy of abundances between these two moving groups and discuss the effects of their chemical evolution and kinematic structures. Section 2 presents the stellar sample and observations. The stellar atmospheric parameters are described in Section 3. Section 4 derives the elemental abundances of our sample stars and estimates the uncertainties while detailed analysis and discussions of the results are given in Section 5. Section 6 summarizes the conclusion of this paper.

2 SAMPLE SELECTION AND OBSERVATIONS

Our observation targets were selected from moving group 6 and 7 (Zhao et al. 2009), primarily depending on the Galactic space-velocity components (U, V, and W). The stars from group 6 have the mean velocity of (38, -20, -15) km s^{-1} while the mean motions of group 7 are (-57, -45, -16) km s^{-1}. These two moving groups have opposite directions of velocities towards the Galactic center, indicating their different locations on the Galactic disk. 19 K-type giants from the two moving groups (9 stars from moving group 6 and 10 stars from moving group 7) were observed. The color-magnitude diagram of our bright and cool sample stars are shown in Figure.1, as well as the whole sample stars from Zhao et al. (2009).

The observations were carried out with BOES (Kim et al. 2007) attached to the 1.8 m telescope at Bohyunsan Optical Astronomy Observatory (BOAO) in two nights: 2009 March 1 and March 4. We used a 2K × 4K CCD with wavelength coverage of 3700 ∼ 9250 Å and set the spectral resolution of BOES to be about 45000, corresponding to the 200 μm fiber. The average signal-to-noise ratio (SNR) of most stars turned out to be in the range of 100 ∼ 200, except for HD44412, which has SNR of 80 due to the bad weather. Figure.2 shows the portions of spectra for two typical stars HD15176 and HD33862.

The spectra were reduced with standard IRAF pipeline for bias subtraction, flat-fielding, scattered-light subtraction, spectral extraction and wavelength calibration. Then we used MIDAS program for continuum normalization. We obtained the radial velocity by cross-correlation method with a standard spectrum. Finally, we calculated the equivalent widths by two methods. For intermediate-strong lines, we fitted the line profiles with a Gaussian function. The direct integration was used for strong unblended lines. We discarded some strong lines (EW > 110 mÅ for FeI lines and EW > 150 mÅ for NiI and CaI lines) which are less sensitive to abundances.

The validity of equivalent width measurements were checked by comparing them to the previous independent work by Takeda et al. (2008), whose spectra were taken from OAO/HIDES, which have resolution of about 67000 and SNR of 100 ∼ 300 for a common star: HD61363 on Figure.3. The systematic differences between the two sets of EW_s are given by a linear least square fitting function with standard deviation of 3.6 mÅ: $EW_{this\ work}$ = 1.13 + 1.016 $EW_{Takeda08}$ (mÅ).

3 STELLAR ATMOSPHERIC PARAMETERS

The effective temperature T_{eff} of our sample stars is determined from the $(B-V)$ and $(V-K)$ photometric data using the empirical calibration relations by Alonso et al. (1999,

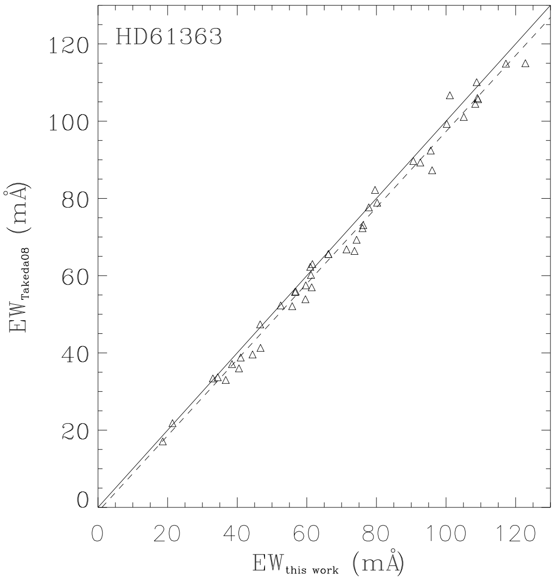

Figure 3. Comparison of equivalent widths measured in this work with Takeda et al. (2008) for the common star. The thick line represents one-to-one relation while the dashed line is the linear fit to the points.

2001). The B, V, K color indices are obtained from SIMBAD database.

We adopt the reddening estimation described by Schlegel et al. (1998); Arce & Goodman (1999); Beers et al. (2002) to obtain the color excess $E(B-V)_A$. For nearby stars, the reddening value is calculated as $E(B-V) = [1-exp(-|Dsinb|/125)]E(B-V)_A$, where D is the distance of the star and b is the Galactic latitude. Then we adopt $E(V-K) = 2.948E(B-V)$ as color excess for $(V-K)$ (Schlegel et al. 1998).

We compare the results derived from $(B-V)$ and $(V-K)$, except for HD26526, which has no K value. The mean difference $< T_{eff}(B-V) - T_{eff}(V-K) >$ is 18 ± 90 K. We also get the excitation equilibrium temperature by forcing a consistent iron abundance derived from different FeI lines with their excitation potentials and compare the results with those obtained from $(V-K)$. The mean difference $< T_{eff}(\mathrm{eq}) - T_{eff}(V-K) >$ is 40 ± 87 K. We plot the results with comparison in Figure.4a, which show no systematic effect between these methods. Table 1 lists T_{eff} derived by photometric and equilibrium methods for our sample stars.

The uncertainty on $T_{eff}(B-V)$ is estimated to be about 100 K according to Alonso et al. (1999). The errors on effective temperature derived from $(V-K)$ mainly come from the uncertainties on K indices which induce the mean error of 105 K, a bit larger than the error estimation given by Alonso et al. (1999). We also estimate the uncertainty on equilibrium temperature to be around 100 K by adding perturbations of T_{eff} to change the slope within a considerable range.

Surface gravity (log g) is determined by:

$$\log g = \log g_{\odot} + \log\,(\frac{M}{M_{\odot}}) + 4\,\log\,(\frac{T_{eff}}{T_{eff,\odot}}) + 0.4(M_{bol} - M_{bol,\odot}) \quad (1)$$

where M is the stellar mass and M_{bol} is the bolometric magnitude.

$$M_{bol} = V + BC + 5\,\log\,\pi + 5 - A_v \qquad (2)$$

where V, BC, π, A_v represent the apparent magnitude, bolometric correction, parallax, and interstellar extinction, respectively. The parallaxes are also taken from SIMBAD. The stellar masses are estimated from Yale-Yonsei stellar evolution tracks (Yi et al. 2003). Interstellar extinction are adopted by $A_v = 3.1E(B-V)$. The bolometric corrections are derived with estimated effective temperatures and metallicities (Alonso et al. 1999).

We also determine log g by forcing FeI and FeII lines to give the same iron abundance. We compare the results between two methods on Figure.4b, the mean difference is 0.10 ± 0.26 dex. Most stars follow the one-to-one relation, while a few stars deviate significantly so that we adopt the latter values for them. The deviation of abundances derived from FeI and FeII lines with adopted log g are plotted in Figure.4c.

The error on the surface gravity comes from the uncertainty on parallaxes and error on mass estimation. The mean uncertainty on log g caused by the relative errors on parallaxes is 0.085 dex for our sample stars. We estimate the uncertainty on stellar mass to be about 0.3 $M\odot$ by comparing the discrepancy between our derived mass with which estimated from the evolution tracks of Girardi et al. (2000), that will induce uncertainty of about 0.12 dex in log g. The overall error on log g is about 0.15 dex, which is consistent with the error estimated by the second method.

The microturbulence, ε_t, is determined by requiring a zero slope relation between $\log A_{\mathrm{Fe}}$ and EW. Only those Fe I lines with 10 mÅ $< EW <$ 110 mÅ are adopted. The uncertainty on microturbulence is estimated to be about 0.2 km s^{-1}.

The initial metallicity for our stars are set to the value of [Fe/H] = 0.0. We adopt the final results by iterating the whole processes of determining the atmospheric parameters T_{eff}, log g, ε_t and [Fe/H] for several times to make them consistent. We also set the original [Fe/H] to -1.0 and repeat the same procedures to check the consistency of the results. A typical difference of final metallicity results is about 0.03 dex for distinct original values. The final adopted stellar parameters for our sample stars are presented in Table 1.

4 ABUNDANCES AND ERROR ESTIMATION

The atomic lines selected for this research cover the spectral range of 5300 ∼ 8000 Å. The loggf values for these lines are taken from some references. Most of our atomic line data are taken from Chen et al. (2000) and Liu et al. (2007). For a few V I lines, the line date are chosen from Allen & Barbuy (2006). We empirically adopt the enhancement factor γ of each element as described by Chen et al. (2000). The atomic line data used for each star are listed in Table 6, which is only available in the electronic version (see the Supplementary Material section). The same atomic line data are adopted to obtain solar abundances and our final results are differential values relative to the Sun.

We calculate the metal abundances with ABONTEST8 program supplied by Dr. Pierre Magain (Liege, Belgium)

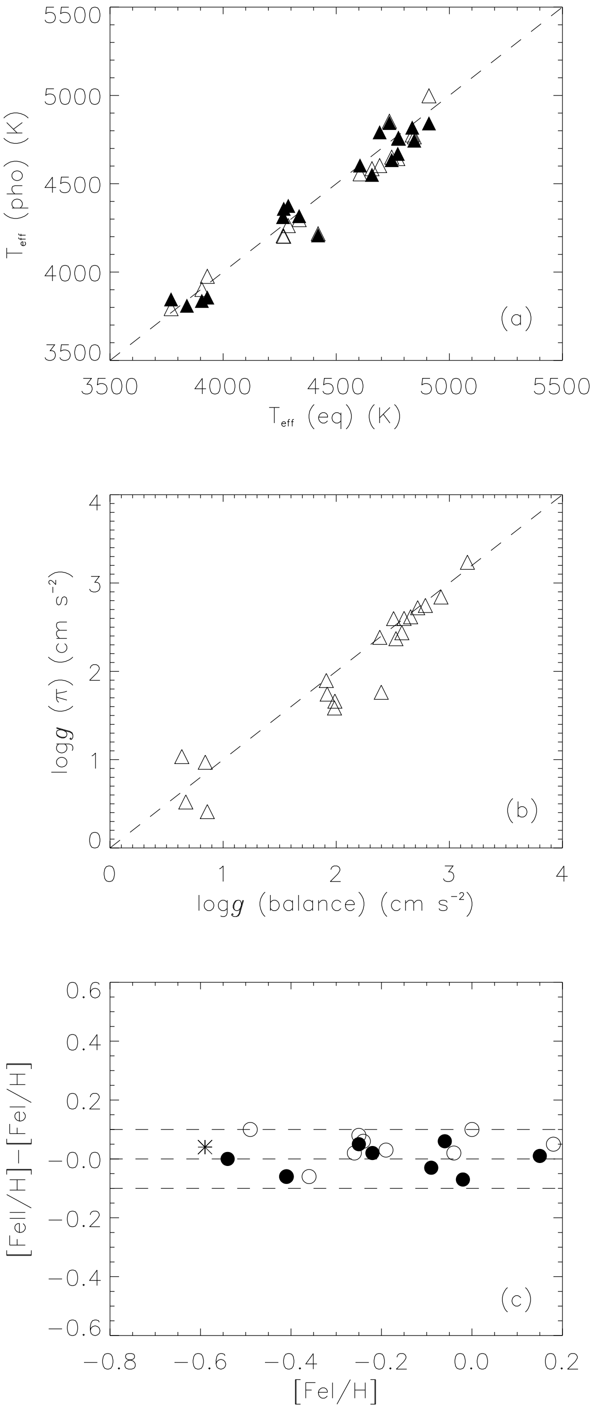

Figure 4. (a): Comparison of effective temperatures derived by photometric and equilibrium methods, filled triangles: $T_{eff}(B-V)$, open triangles: $T_{eff}(V-K)$. (b): Comparison of surface gravities derived by parallaxes and ionization balance of FeI and FeII lines. (c): Abundance deviations derived from FeII and FeI lines versus metallicity, filled circles: moving group 6, open circles: moving group 7, asterisk: HD44412.

Table 1. Stellar parameters of sample stars.

	derived T_{eff}			adopted parameters			
HD	T_{eff}^{B-V}	T_{eff}^{V-K}	T_{eff}^{eq}	T_{eff}	log g	ε_t	[Fe/H]
15176	4604	4556	4605	4556	2.437	1.3	-0.09
26526	3810	· · ·	3840	3810	0.521	1.3	-0.54
33862	4818	4776	4836	4776	2.599	1.4	-0.25
34303	4845	4854	4735	4735	3.160	1.1	0.15
40331	4375	4263	4288	4263	1.896	1.5	-0.22
44412	3846	3792	3770	3770	0.635	1.9	-0.59
48073	4842	4998	4910	4910	2.720	1.5	-0.02
67174	3856	3976	3930	3930	0.860	1.5	-0.41
80130	4745	4765	4845	4765	2.746	1.4	-0.06
39723	4209	4217	4420	4217	1.763	1.5	-0.04
45192	4359	4202	4268	4202	1.742	1.5	-0.26
51397	4551	4585	4658	4585	2.369	1.5	-0.19
61363	4792	4603	4692	4692	2.385	1.3	-0.25
71704	4756	4757	4775	4775	2.507	1.4	-0.24
75556	4312	4204	4265	4204	1.662	1.3	-0.36
82104	3837	3902	3906	3902	0.971	1.5	-0.49
85425	4670	4642	4772	4772	2.926	1.3	0.18
90250	4634	4650	4745	4650	2.618	1.4	0.00
95463	4317	4297	4336	4336	1.985	1.5	-0.41

Table 2. Comparison of stellar parameters between this work and previous studies for common stars.

	this work			previous work		
HD	T_{eff}	log g	[Fe/H]	T_{eff}	log g	[Fe/H]
15176 [a]	4556	2.437	-0.09	4540	2.63	-0.19
61363 [b]	4692	2.385	-0.25	4762	2.33	-0.31
90250 [c]	4650	2.618	0.00	4639	2.35	-0.10

[a] McWilliam (1990); [b] Takeda et al. (2008); [c] Schiavon (2007).

based on the homogeneous, plane-parallel and local thermodynamic equilibrium models by Castelli & Kurucz (2003). The program matches observed EWs with theoretical values calculated based on the atmospheric model. It takes into account natural broadening, van der Waals damping broadening and thermal broadening.

We check the consistency of the stellar parameters with previous studies (McWilliam 1990; Schiavon 2007; Takeda et al. 2008) for three common stars. The comparison of the effective temperature, gravity and metallicity of these stars is given in Table 2. The mean deviation of effective temperature $\triangle T_{eff}$ is about 14.3 ± 51.4 K lower than others' results. While the gravity difference $\triangle$log g is about 0.04 ± 0.24 dex being higher compared with others. Our metallicity presents systematically 0.09 ± 0.11 dex higher than those from literature values, which is within the error on parameters. Comparing with the results of Takeda et al. (2008), our metallicity of a comment star HD61363 is a bit higher by the order of 0.06 dex, which may come from the deviation values of EWs and microturbulence.

We derive the [X/Fe] ratios of 12 elements (Al, Ba, Ca, K, Mg, Mn, Na, Ni, Sc, Si, Ti and V) and plot the trends in Figure.5 to Figure.7, together with previous works of Liu et al. (2007), hereafter Liu07 and Takeda et al. (2008), hereafter Takeda08 as comparison. We note that for HD44412, most of results deviate seriously from others due to much lower SNR of it's spectrum and it is the coolest star

Table 3. HFS line list.

Ion	λ (Å)	EP (eV)	log gf	Ion	λ (Å)	EP (eV)	log gf	Ion	λ (Å)	EP (eV)	log gf
BaII	6141.695	0.70	-3.177	ScII	5526.787	1.77	-1.921	ScII	6604.609	1.36	-2.708
BaII	6141.697	0.70	-2.063	ScII	5526.788	1.77	-1.185	ScII	6604.611	1.36	-2.506
BaII	6141.698	0.70	-3.039	ScII	5526.789	1.77	-0.523	ScII	6604.613	1.36	-2.348
BaII	6141.699	0.70	-1.176	ScII	5526.790	1.77	-1.180	ScII	6604.615	1.36	-2.136
BaII	6141.700	0.70	-0.166	ScII	5526.791	1.77	-0.644	V I	5737.045	1.06	-1.307
BaII	6141.701	0.70	-1.366	ScII	5526.792	1.77	-1.368	V I	5737.055	1.06	-1.380
BaII	6141.702	0.70	-1.639	ScII	5526.793	1.77	-0.712	V I	5737.063	1.06	-1.467
BaII	6141.703	0.70	-2.229	ScII	5526.794	1.77	-0.936	V I	5737.069	1.06	-1.576
BaII	6496.888	0.60	-2.836	ScII	5526.795	1.77	-0.854	V I	5737.074	1.06	-1.722
BaII	6496.889	0.60	-3.058	ScII	5657.886	1.51	-1.126	V I	5737.077	1.06	-1.944
BaII	6496.891	0.60	-2.132	ScII	5657.888	1.51	-1.696	V I	6090.199	1.08	-0.690
BaII	6496.892	0.60	-2.367	ScII	5657.893	1.51	-1.696	V I	6090.207	1.08	-0.831
BaII	6496.896	0.60	-1.486	ScII	5657.894	1.51	-1.524	V I	6090.213	1.08	-0.884
BaII	6496.900	0.60	-0.466	ScII	5657.895	1.51	-1.538	V I	6090.218	1.08	-0.957
BaII	6496.906	0.60	-2.331	ScII	5657.899	1.51	-1.538	V I	6090.223	1.08	-1.055
BaII	6496.907	0.60	-2.367	ScII	5657.901	1.51	-2.219	V I	6090.225	1.08	-2.645
BaII	6496.908	0.60	-2.132	ScII	5657.902	1.51	-1.549	V I	6090.226	1.08	-1.302
BaII	6496.910	0.60	-2.367	ScII	5657.904	1.51	-1.549	V I	6090.227	1.08	-1.837
BaII	6496.912	0.60	-2.132	ScII	5657.906	1.51	-1.717	V I	6090.228	1.08	-2.234
MnI	6016.619	3.07	-1.360	ScII	5657.908	1.51	-1.722	V I	6090.229	1.08	-1.393
MnI	6016.645	3.07	-1.197	ScII	5657.909	1.51	-1.898	V I	6090.231	1.08	-1.444
MnI	6016.647	3.07	-0.582	ScII	5684.190	1.51	-1.473	V I	6090.232	1.08	-1.887
MnI	6016.667	3.07	-1.192	ScII	5684.191	1.51	-1.962	V I	6090.233	1.08	-1.549
MnI	6016.668	3.07	-0.845	ScII	5684.193	1.51	-2.660	V I	6274.607	0.27	-2.932
MnI	6016.684	3.07	-1.176	ScII	5684.204	1.51	-1.766	V I	6274.629	0.27	-2.455
MnI	6016.685	3.07	-1.294	ScII	5684.205	1.51	-1.846	V I	6274.641	0.27	-2.476
MnI	6016.696	3.07	-1.171	ScII	5684.206	1.51	-2.221	V I	6274.655	0.27	-2.134
MnI	6016.698	3.07	-1.556	ScII	5684.215	1.51	-2.221	V I	6274.657	0.27	-2.455
MnI	6016.704	3.07	-2.319	ScII	5684.216	1.51	-1.966	V I	6274.678	0.27	-2.601
MnI	6016.707	3.07	-1.197	ScII	5684.217	1.51	-1.950	V I	6285.098	0.28	-3.570
MnI	6016.713	3.07	-1.192	ScII	6245.621	1.51	-1.602	V I	6285.117	0.28	-3.141
MnI	6016.714	3.07	-1.556	ScII	6245.629	1.51	-2.342	V I	6285.122	0.28	-2.703
MnI	6016.716	3.07	-1.294	ScII	6245.631	1.51	-1.773	V I	6285.134	0.28	-2.890
MnI	6021.746	3.07	-2.659	ScII	6245.636	1.51	-3.347	V I	6285.137	0.28	-2.542
MnI	6021.772	3.07	-1.445	ScII	6245.638	1.51	-2.159	V I	6285.148	0.28	-2.714
MnI	6021.774	3.07	-2.307	ScII	6245.640	1.51	-1.980	V I	6285.149	0.28	-2.550
MnI	6021.795	3.07	-1.269	ScII	6245.644	1.51	-2.924	V I	6285.152	0.28	-2.077
MnI	6021.798	3.07	-2.182	ScII	6245.646	1.51	-2.126	V I	6285.157	0.28	-2.714
MnI	6021.804	3.07	-0.527	ScII	6245.647	1.51	-2.251	V I	6285.162	0.28	-2.293
MnI	6021.813	3.07	-1.243	ScII	6245.650	1.51	-2.690	V I	6285.168	0.28	-2.576
MnI	6021.817	3.07	-2.261	ScII	6245.651	1.51	-2.185	V I	6285.172	0.28	-3.014
MnI	6021.821	3.07	-0.667	ScII	6245.652	1.51	-2.670	V I	6452.309	1.19	-2.414
MnI	6021.827	3.07	-1.310	ScII	6245.655	1.51	-2.544	V I	6452.312	1.19	-2.414
MnI	6021.834	3.07	-0.825	ScII	6245.656	1.51	-2.368	V I	6452.316	1.19	-2.714
MnI	6021.837	3.07	-1.486	ScII	6245.657	1.51	-2.447	V I	6452.319	1.19	-2.590
MnI	6021.843	3.07	-1.009	ScII	6604.582	1.36	-2.506	V I	6452.323	1.19	-2.250
MnI	6021.846	3.07	-1.516	ScII	6604.590	1.36	-2.348	V I	6452.328	1.19	-2.276
MnI	6021.847	3.07	-1.231	ScII	6604.594	1.36	-1.936	V I	6452.333	1.19	-2.841
ScII	5526.770	1.77	-2.666	ScII	6604.596	1.36	-2.359	V I	6452.338	1.19	-2.242
ScII	5526.775	1.77	-2.257	ScII	6604.599	1.36	-2.334	V I	6452.345	1.19	-1.993
ScII	5526.779	1.77	-1.354	ScII	6604.602	1.36	-2.532	V I	6452.351	1.19	-3.270
ScII	5526.783	1.77	-1.167	ScII	6604.604	1.36	-3.029	V I	6452.357	1.19	-2.403
ScII	5526.786	1.77	-1.181	ScII	6604.607	1.36	-4.465	V I	6452.365	1.19	-1.777

in our sample. So we analyze our results without considering this star's value.

The hyper fine structure (HFS) effect has been considered for Ba, Mn, Sc and V elements. The adopted HFS data are taken from McWilliam (1998) and Kurucz[1], as presented in Table 3. The largest HFS correction is about 0.18 dex for [Ba/Fe], -0.35 dex for [Mn/Fe] and -0.08 dex for [Sc/Fe]. For V element, the HFS effect can lead to a correction as large as -0.55 dex, consistent with Liu07. The discrepancy of elemental abundances resulting from HFS correction for these elements exhibit decreasing trends with increasing metallicity, as shown in Figure.5. We adopt the results of [Ba/Fe], [Mn/Fe], [Sc/Fe] and [V/Fe] with HFS correction.

---

[1] http://kurucz.harvard.edu/linelists.html

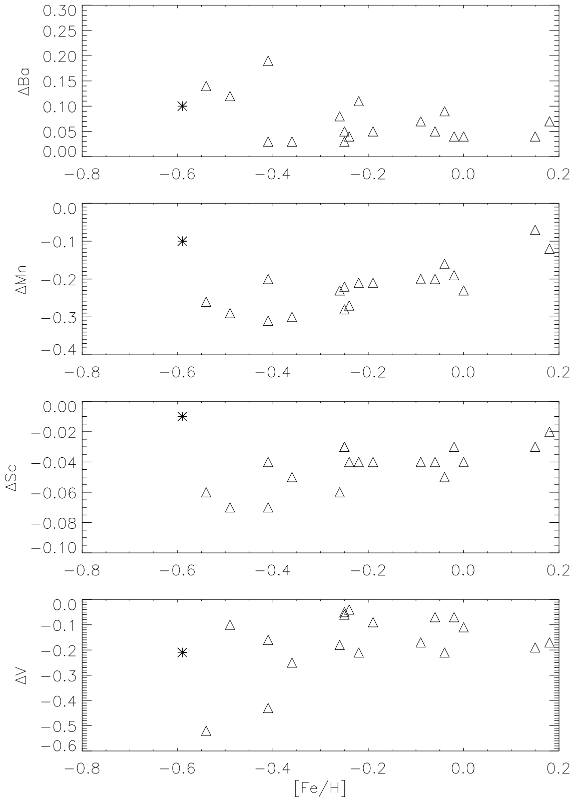

Figure 5. The abundance deviations for Ba, Mn, Sc and V, obtained by considering HFS effect minus those by neglecting HFS versus [Fe/H], asterisk: HD44412.

We estimate the uncertainties on abundances for our sample stars from two sources. One is the internal error due to the scatter of our abundance results from individual lines. This error is calculated by dividing the standard deviation of derived abundances by a square root of the numbers of lines used ($\sqrt{N}$). Another error comes from the stellar atmospheric parameters. The effects on the derived abundances are estimated by changing the atmospheric parameters. Table 4 presents the abundance deviations due to a change by 100 K in effective temperature, 0.15 dex in surface gravity, 0.2 km s^{-1} in microturbulence, and 0.1 dex in metallicity, along with the internal error ($\frac{\sigma_{EW}}{\sqrt{N}}$), for a typical star HD33862 in our sample. The uncertainties on abundances for most chemical elements are less than 0.1 dex.

5 RESULTS AND DISCUSSIONS

5.1 Abundances between upper red giants and red clump giants

Most of our sample stars belong to upper red giants, which have brighter absolute magnitude with cooler effective temperature than red clump giants, are influenced by stellar evolution more seriously. We analyze our results of elemental abundances, compared with the work of Liu07 and Takeda08 on red clump giants. We find that most chemical elements show similar abundance trends with a few exceptions of Al, Na and Ba, on which evolution effects contribute significantly. We plot [X/Fe] of Mn, Ni, V, Ca, Mg, Si, Ti, K and Sc versus [Fe/H] in Figure.6, and the trends of Al, Na and Ba are shown in Figure.7. The abundance ratios of these elements for our sample stars are listed in Table 5.

The iron-peak elements are believed to have the same patterns as iron. [Mn/Fe] increase with higher metallicity in our work, which is well consistent with Takeda08. The trend of [Ni/Fe] are flat with -0.6 < [Fe/H] < 0.2 for our stars. Our results of [Ni/Fe] show systematic higher ($\sim$ 0.05 dex) than the work of Takeda08, but our results are well consistent with Liu07. The [V/Fe] values show larger scatter for some of our stars with relative lower effective temperature, because V I lines are very sensitive to temperature (Allen & Barbuy 2006). Moreover, the V I lines of those stars are so strong that it may be contaminated by other lines.

The α elements are primarily produced by SN II nucleosynthesis and exhibit enrichment in metal-poor stars (Woosley & Weaver 1995). All these elements show increments towards lower metallicity and exhibit turn off trends to flatter patterns at [Fe/H] $\sim$ -0.2 with slightly differences, which are in good agreement with previous studies of Takeda08 and Liu07. We notice that the trend of [Mg/Fe] is steeper than other α elements and our results of [Ti/Fe] show a bit larger scatter.

For odd-Z light elements, [K/Fe] exhibits a larger dispersion as reported by Wang et al. (2011), because only one strong line is available. We divide our stellar spectra by the spectrum of B-type star HD5394 observed in the same night to check the effect of H_2O lines. We find no change of our results that demonstrate insignificant influence of H_2O lines for our K I line. [Sc/Fe] shows a flat pattern, which is consistent with Takeda08. [Al/Fe] decreases with increasing metallicity for [Fe/H] < -0.2, and becomes flat towards higher metallicity. Although the trend of [Al/Fe] is similar with Liu07, our results are richer at [Fe/H] < -0.4. [Na/Fe] also shows enrichment at [Fe/H] < -0.4, which may be due to stellar evolution effects. For other stars, the trend of [Na/Fe] is consistent with Takeda08 and Liu07.

Barium is produced mainly by *s* process, which can be used as the stellar evolution tracer. We consider that there is a turn off at [Fe/H] $\sim$ -0.2 on the trend of [Ba/Fe] versus [Fe/H], which is consistent with Chen et al. (2000) and Liu07. Yet our results of [Ba/Fe] show enrichment at [Fe/H] < -0.4, that indicate those stars are affected seriously by evolution process.

5.2 Abundances analysis of Na, Al, Mg and Ba

Na and Al are thought to be produced in SNe II and SNe Ib/c (Nomoto et al. 1984), different relative to the production of Mg. The cycle of Na-Al-Mg is crucial to nucleosynthesis on our results since they can partly reflect the chemical evolution histories of our giants. We plot the abundances of Na and Al relative to Mg versus [Mg/H] in Figure.8 with comparison with work by Luck & Heiter (2007), hereafter LH07 and Liu07 without NLTE correction, since Mg can be seen as a better metallicity tracer (Cayrel et al. 2004). Our results of [Na/Mg] increase smoothly with higher [Mg/H], which can be fitted by the relation of [Na/Mg] = 0.007 +

Table 4. Estimated errors on elemental abundances for HD33862.

Δ	$\frac{\sigma_{EW}}{\sqrt{N}}$	ΔT_{eff} (+100K)	$\Delta \log g$ (+0.15)	$\Delta\varepsilon_t$ (+0.2)	Δ[Fe/H] (+0.1)	σ_{Total}
Δ[FeI/H]	0.008	-0.060	-0.013	0.067	-0.012	0.092
Δ[FeII/H]	0.027	0.087	-0.078	0.057	-0.040	0.139
Δ[AlI/Fe]	0.070	0.001	0.022	-0.053	0.010	0.091
Δ[BaII/Fe]	0.001	0.007	0.003	0.048	-0.045	0.066
Δ[CaI/Fe]	0.034	-0.039	0.034	0.019	0.011	0.066
Δ[K I/Fe]	$\cdots^{a}$	-0.057	0.054	0.032	0.005	0.085
Δ[MgI/Fe]	0.018	0.006	0.031	-0.023	0.002	0.043
Δ[MnI/Fe]	0.030	-0.049	0.041	0.056	-0.013	0.091
Δ[NaI/Fe]	0.013	-0.023	0.030	-0.022	0.010	0.047
Δ[NiI/Fe]	0.014	0.010	-0.004	0.021	-0.010	0.029
Δ[ScII/Fe]	0.028	0.066	-0.045	0.018	-0.024	0.090
Δ[SiI/Fe]	0.026	0.074	-0.014	-0.034	-0.009	0.087
Δ[TiI/Fe]	0.047	-0.072	0.015	-0.030	0.012	0.093
Δ[TiII/Fe]	$\cdots^{a}$	0.065	-0.045	0.067	-0.021	0.106
Δ[V I/Fe]	0.032	-0.108	0.012	-0.008	0.018	0.115

[a] Only one line is available.

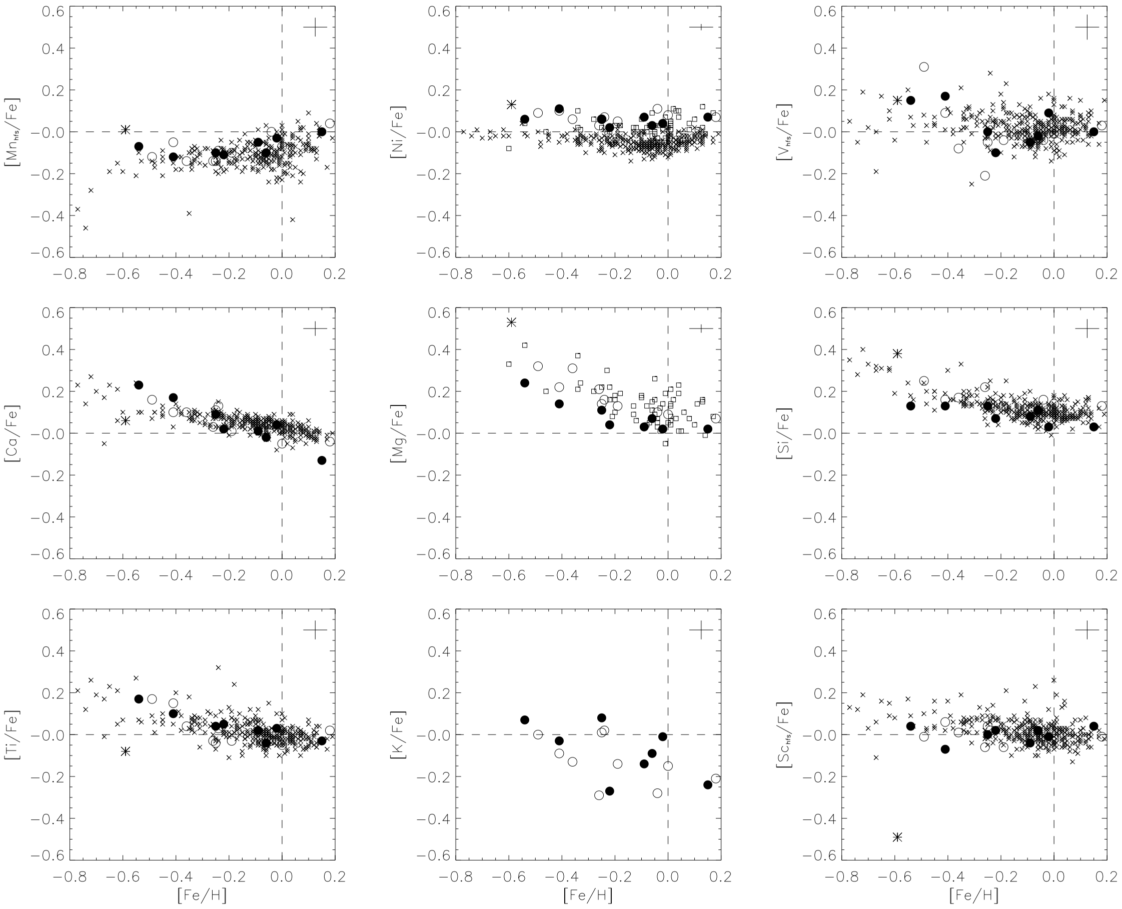

Figure 6. Abundance ratio [X/Fe] for Mn, Ni, V, Ca, Mg, Si, Ti, K and Sc versus [Fe/H]. Filled circles: moving group 6, open circles: moving group 7, asterisk: HD44412, crosses: Takeda et al. (2008), rectangles: Liu et al. (2007).

Table 5. Stellar abundance ratios [X/Fe].

HD	[Al/Fe]	[Ba/Fe]	[Ca/Fe]	[K/Fe]	[Mg/Fe]	[Mn/Fe]	[Na/Fe]	[Ni/Fe]	[Sc/Fe]	[Si/Fe]	[Ti/Fe]	[V/Fe]
15176	0.13	0.26	0.01	-0.14	0.03	-0.05	0.09	0.07	-0.04	0.08	0.02	-0.05
26526	0.33	0.49	0.23	0.07	0.24	-0.07	0.35	0.06	0.04	0.13	0.17	0.15
33862	0.16	0.15	0.09	0.08	0.11	-0.10	0.12	0.06	-0.00	0.13	0.04	-0.00
34303	0.06	0.05	-0.13	-0.24	0.02	-0.00	0.09	0.07	0.04	0.03	-0.03	-0.00
40331	0.08	0.40	0.02	-0.27	0.04	-0.11	0.09	0.02	0.02	0.07	0.05	-0.10
44412	0.75	0.17	0.06	· · ·	0.53	0.01	0.32	0.13	-0.49	0.38	-0.08	0.15
48073	0.15	0.26	0.04	-0.01	0.02	-0.03	0.20	0.04	-0.01	0.03	0.03	0.09
67174	0.22	0.61	0.17	-0.03	0.14	-0.12	0.16	0.11	-0.07	0.13	0.10	0.17
80130	0.10	0.28	-0.02	-0.09	0.07	-0.10	0.05	0.03	0.02	0.11	-0.04	-0.02
39723	0.19	0.35	0.04	-0.28	0.10	-0.00	0.24	0.11	-0.05	0.16	-0.03	-0.04
45192	0.21	0.23	0.03	-0.29	0.21	-0.14	0.15	0.03	-0.06	0.22	-0.03	-0.21
51397	0.24	0.19	0.01	-0.14	0.13	-0.10	0.11	0.05	-0.06	0.13	-0.03	-0.04
61363	0.12	0.28	0.11	0.01	0.14	-0.14	0.17	0.06	0.04	0.14	-0.04	-0.05
71704	0.19	0.18	0.13	0.02	0.16	-0.09	0.09	0.07	0.02	0.14	0.03	0.03
75556	0.29	0.05	0.10	-0.13	0.31	-0.14	0.12	0.06	0.01	0.17	0.04	-0.08
82104	0.46	0.35	0.16	0.00	0.32	-0.12	0.32	0.09	-0.01	0.25	0.17	0.31
85425	0.06	0.12	-0.04	-0.21	0.07	0.04	0.11	0.07	-0.01	0.13	0.02	0.03
90250	0.10	0.10	-0.05	-0.15	0.09	-0.07	0.08	0.08	-0.02	0.14	-0.05	-0.01
95463	0.27	0.08	0.10	-0.09	0.22	-0.05	0.15	0.10	0.06	0.16	0.15	0.09

Note: HFS corrections have been adopted for [Ba/Fe], [Mn/Fe], [Sc/Fe] and [V/Fe].

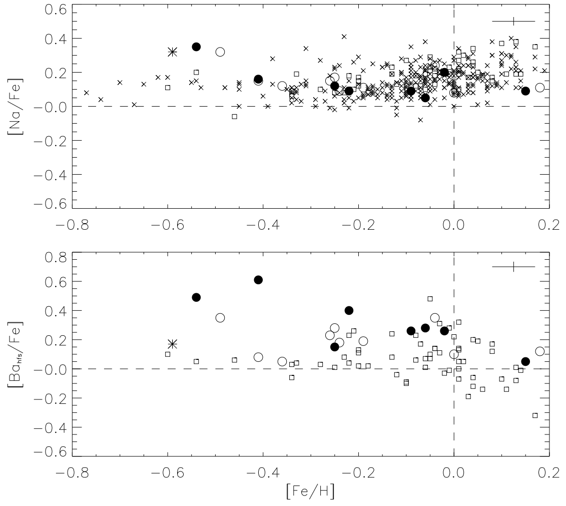

Figure 7. Abundance ratio [X/Fe] for Al, Na and Ba versus [Fe/H]. Filled circles: moving group 6, open circles: moving group 7, asterisk: HD44412, crosses: Takeda et al. (2008), rectangles: Liu et al. (2007).

0.064 [Mg/H], while the results of Liu07 show steeper increasing trend. Results of LH07 show larger scatter so that we can hardly find explicit relation. Our results of [Na/Mg] display overabundance at lower [Mg/H], with respect to that of Liu07, for those stars which have evolved to upper-tip red giant branch. The reason is that the abundance of Na will be enriched as a result of Ne-Na cycle from deeper layers being dredged to the surface, and has also been found in some studies of giants (Andrievsky et al. 2002; Mishenina et al. 2006). Our results of [Al/Mg] decrease slightly with increasing [Mg/H], which have the relation of [Al/Mg] = 0.054 - 0.116 [Mg/H], different with the trend of Liu07 but consistent with that of LH07, may also due to the effects of evolution since the sample of LH07 has wider range of evolution than that of Liu07. The trends of Na-Al-Mg indicate that Mg abundances are less affected by possible nucleosynthesis and mixing than that of Na or Al (Langer et al. 1993).

We find that our results of most elemental abundances are in good agreements between moving group 6 and 7, only except for Mg and Ba elements. [Mg/Fe] of moving group 7 stars are a bit higher (∼ 0.04 dex) than the results of stars from moving group 6. We also notice that [Ba/Fe] values of moving group 7 stars are a bit smaller (∼ 0.10 dex) than that of moving group 6 stars, which is in contrast with the results of [Mg/Fe]. The trends of [Ba/Fe] versus metallicity for two moving group stars show discrepancy too. The contrast trends of Mg and Ba demonstrate that these two elements are predominantly synthesized in different progenitor mass ranges (Arnone et al. 2005).

Considered that [Ba/H] is a better indicator for investigating evolution effect, we plot the abundance ratio [Mg/Ba] versus [Ba/H] in Figure.9, which shows the decreasing trend of [Mg/Ba] with higher [Ba/H] for both moving groups, representing the anticorrelation of abundances between Ba and Mg. We compare our results with the work of Allen & Barbuy (2006), whose sample include giants, subgiants and dwarfs for barium-rich stars to investigate the

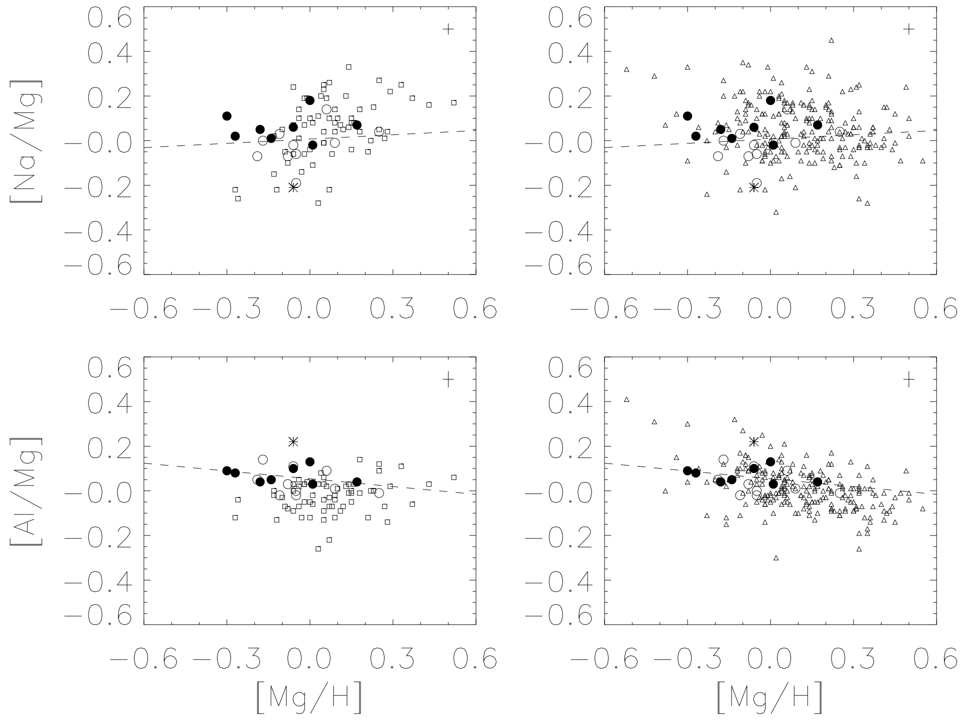

Figure 8. Abundance ratio [Na/Mg] and [Al/Mg] versus [Mg/H]. Left panel: comparison with Liu et al. (2007), right panel: comparison with Luck & Heiter (2007). Filled circles: moving group 6, open circles: moving group 7, asterisk: HD44412, rectangles: Liu et al. (2007), triangles: Luck & Heiter (2007).

effect of evolution better. Although the ranges of [Ba/H] are different in these two samples, the trend of [Mg/Ba] versus [Ba/H] shows consistency which can be well fitted by a linear relation of [Mg/Ba] = -0.116 - 1.184 [Ba/H], based on data of Allen & Barbuy (2006) and our results. The reason is that probable *s* process sites are the atmospheres of stars on the AGB stars (Busso et al. 1999), which is different from that of Mg element, essentially all produced by SN II explosion. Although our sample stars are not barium rich stars, the evolution effect can be reduced by comparison of stars with similar [Ba/H] ratios. We notice that the values of [Mg/Ba] are higher for moving group 7 stars than stars of moving group 6, as shown in the box region of Figure.9. Such differences may indicate distinct chemical evolution traces of these two moving groups.

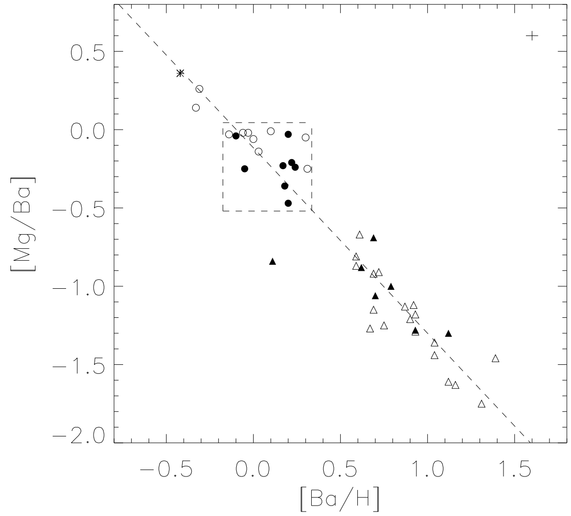

Figure 9. Abundance ratio [Mg/Ba] versus [Ba/H]. Filled circles: moving group 6, open circles: moving group 7, asterisk: HD44412, filled triangles: stars with log $g < 3.0$ from Allen & Barbuy (2006), open triangles: other stars from the same literature.

5.3 Kinematic analysis

To further investigate the origins and evolution traces of moving groups 6 and 7, it is valuable to carefully analyze our abundance results of some chemical elements with dynamical effects. The kinematical parameters of our sample stars are taken from Famaey et al. (2005). Stars of moving group 7 have smaller values of minimum Galactocentric distance (R_{min}) and higher mean height towards Galactic disk (Z_{max}) than those of moving group 6, corresponding to their larger Galactic velocity of (U, V) values as described by Nordström et al. (2004). We plot the abundance ratios of [Mg/Ba] for our stars with kinematical parameters of R_{min} and Z_{max} in Figure.10 to analyze the abundances discrepancy between moving group 6 and 7 which have opposite

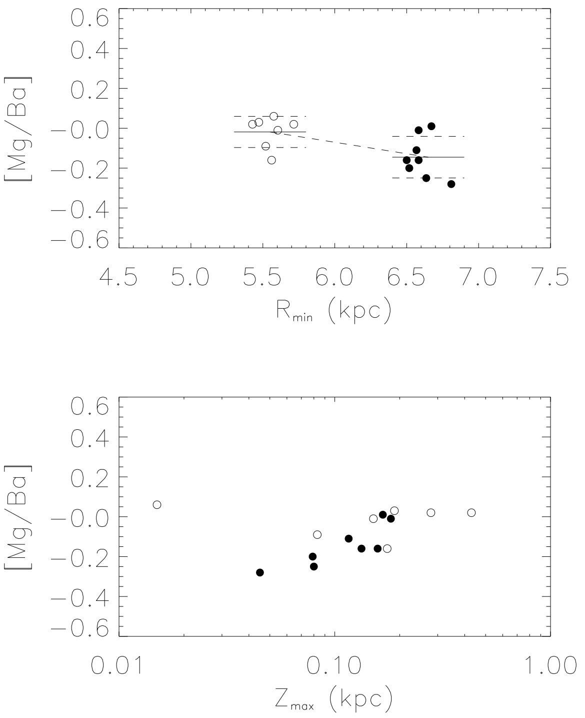

Figure 10. Abundance ratio [Mg/Ba] versus R_{min} and Z_{max}. Filled circles: moving group 6, open circles: moving group 7.

U-velocity. We select stars carefully from the box area with [Ba/H] ∼ 0 in Figure.9 to reduce the effects of stellar evolution and find that the mean value of [Mg/Ba] is -0.072 ± 0.090 for moving group 7 and -0.229 ± 0.147 for moving group 6, with the discrepancy of about 0.16 dex, which may hint the kinematics from their different R_{min} (see Figure.10). The scatter of the results are a bit larger for moving group 6, which show dependences on Z_{max}. In spite of that, the distinction of [Mg/Ba] between these two moving groups can not be eliminated by other factors so that we can set the conclusion elaborately that such abundance discrepancy may indicate the different chemical synthesis histories of both moving groups. We find no explicit relations of Mg and Ba abundances with different Z_{max}.

We plot [Fe/H] distributions with the mean Galactocentric distances (R_g) in Figure.11, together with previous studies on open clusters (Friel et al. 2002; Yong et al. 2005; Bragaglia et al. 2008; Pancino et al. 2010) as comparison. The metallicity of our stars from each moving group cover a wider range than that of open clusters at $R_g \sim 7.5$ kpc. The values of [Fe/H] spread out to about -0.5 dex for our sample, which is different from that of open clusters with -0.2 < [Fe/H] < 0.2. The metallicity scatter of our sample stars from moving group 6 and 7 are 0.22 and 0.20 dex, which are much larger than those of open clusters with scatter less than 0.05 dex. Such wider metallicity range and larger abundance scatter point out chemical inhomogeneity of moving group 6 and 7, although each of them has kinematic coherence in the velocity space. The inhomogeneity of these two moving groups, different from open clusters, may indicate that the stars of moving group 6 and 7 have different chemical origins before they were kinematically gathered and both moving groups are not the dispersed remnants of clusters or star-forming events, but rather result from the kinematic effects of the Galactic spiral structure so that we would not expect these kinematic groups to be chemically homogeneous and coeval. Our results of moving group 6 and 7, which show distinct behaviors with respect to open clusters, support the hypothesis with mechanisms of dynamical resonance.

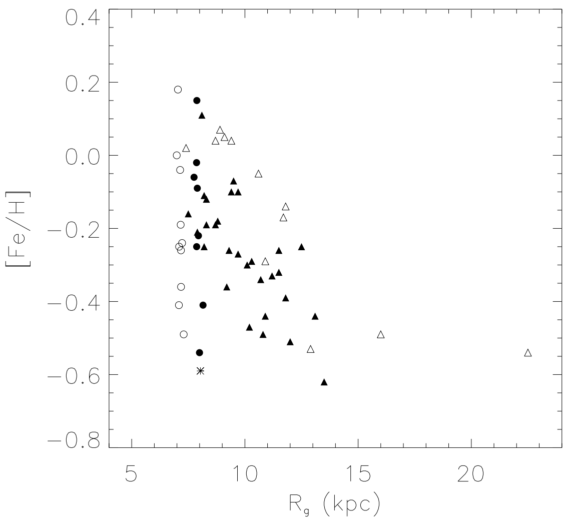

Figure 11. [Fe/H] versus R_g. Filled circles: moving group 6, open circles: moving group 7, asterisk: HD44412, filled triangles: Friel et al. (2002), open triangles: Yong et al. (2005); Bragaglia et al. (2008); Pancino et al. (2010).

6 CONCLUSION

In this work we determine the stellar atmospheric parameters and chemical abundances of 19 K-type giants from moving group 6 and 7, which have anti-U velocity towards Galactic center, based on high resolution spectra obtained at BOAO, covering the metallicity range -0.6 < [Fe/H] < 0.2. From the results of abundances combined with kinematical parameters, we conclude that abundances of most elements show similar trends with previous studies on giants (Liu07; Takeda08) except for Al, Na and Ba, because of evolution effects on our upper red giants. The iron-peak elements have the same patterns as iron. α elements — Ca, Mg, Si, Ti exhibit increasing trends towards lower metallicity and show the turn off trends to flatter patterns at [Fe/H] ∼ -0.2. [K/Fe] exhibits a larger dispersion while [Sc/Fe] shows flat solar pattern. The abundances of Al, Na and Ba exhibit overabundances at [Fe/H] < -0.4 for the more evolved stars.

Our results of [Na/Mg] increase smoothly with higher [Mg/H] and [Al/Mg] decrease slightly with increasing [Mg/H], which are affected by stellar internal evolution significantly. The abundance ratios [Mg/Ba] of moving group 6 and 7 stars with similar [Ba/H] ∼ 0 are distinct by the order of 0.16 dex, which could come from their distinct chemical evolution histories corresponding to their different kinematics. The inhomogeneous [Fe/H] values of these two moving group stars present different chemical origins for stars from both moving groups and favor the dynamical resonant theory. Future works need to be done by enlarging the sample of stars and spreading out to other moving groups to further investigate the origins and evolution of these kinematic structures in the Galaxy.

ACKNOWLEDGMENTS

FL is grateful of Drs. Y. J. Liu, H. N. Li, L. Wang and Ms. S. Liu for their valuable advices and discussions. This work is supported by the National Natural Science Foundation of China under grant number 11073026, 11173031.

REFERENCES

Allen D.M., Barbuy B., 2006, A&A, 454, 895
Alonso A., Arribas S., Martìnez-Roger C., 1999, A&AS, 140, 261
Alonso A., Arribas S., Martìnez-Roger C., 2001, A&A, 376, 1039
Andrievsky S.M., Egorova I.A., Korotin S.A., Burnage R., 2002, A&A, 389, 519
Antoja T., Figueras F., Fernandez D., Torra J., 2008, A&A, 490, 135
Arce H.G., Goodman A.A., 1999, ApJ, 512, L135
Arnone E., Ryan S.G., Argast D., Norris J.E., Beers T.C., 2005, A&A, 430, 507
Beers T.C., Drilling J.S., Rossi S., Chiba M., Rhee J., Führmeister B., Norris J.E., von Hippel T., 2002, AJ, 124, 931
Bragaglia A., Sestito P., Villanova S., Carretta E., Randich S., Tosi M., 2008, A&A, 480, 79
Busso M., Gallino R., Wasserburg G.J., 1999, ARA&A, 37, 239
Castelli F., Kurucz R.L., 2003, IAU Symposium, 210, 20
Cayrel R., Depagne E., Spite M., Hill V., Spite F., François P., Plez B., Beers T., Primas F., Andersen J., Barbuy B., Bonifacio P., Molaro P., Nordström B., 2004, A&A, 416, 1117
Chen B., Asiain R., Figueras F., Torra J., 1997, A&A, 318, 29
Chen Y.Q., Nissen P.E., Zhao G., Zhang H.W., Benoni T., 2000, A&AS, 141, 491
Dehnen W., 1998, AJ, 115, 2384
De Silva G.M., Freeman K.C., Bland-Hawthorn J., Asplund M., Bessell M.S., 2007, AJ, 133, 694
Eggen O.J., 1996, ApJ, 112, 1595
ESA, 1997, The Hipparcos and Tycho Catalogues, ESA SP-1200
Famaey B., Jorissen A., Luri X., Mayor M., Udry S., Dejonghe H., Turon C., 2005, A&A, 430, 165
Famaey B., Pont F., Luri X., Mayor M., Jorissen A., 2007, A&A, 461, 957
Famaey B., Siebert A., Jorissen A., 2008, A&A, 483, 453
Friel E.D., Janes K.A., Tavarez M., Scott J., Katsanis R., Lotz J., Hong L., Miller N., 2002, AJ, 124, 2693
Girardi L., Bressan A., Bertelli G., Chiosi C., 2000, A&AS, 141, 371
Helmi A., Navarro J.F., Nordström B., Holmberg J., Abadi M.G., Steinmetz M., 2006, MNRAS, 365, 1309
Kalnajs A.J., 1991, Dynamics of Disk Galaxies, ed. B. Sundelius, 323
Kim K.-M., Han I., Valyavin G.G., Plachinda S., Jang J.G., Jang B.-H., Seong H.C., Lee B.-C., Kang D.-I., Park B.-G., Yoon T.S., Vogt S.S., 2007, PASP, 119, 1052
Klement R., Fuchs B., Rix H.W., 2008, ApJ, 685, 261
Langer G.E., Hoffman R., Sneden C., 1993, PASP, 105, 301
Liu Y.J., Zhao G., Shi J.R., Pietrzyǹski G., Gieren W., 2007, MNRAS, 382,553
Luck R.E., Heiter U., 2007, AJ, 133, 2464
Mayor M., 1972, A&A, 18, 97
McWilliam A., 1990, ApJS, 74, 1075
McWilliam A., 1998, AJ, 115, 1640
Mishenina T.V., Bienaymé O., Gorbaneva T.I., Charbonnel C., Soubiran C., Korotin S.A., Kovtyukh V.V., 2006, A&A, 456, 1109
Nomoto K., Thielemann F.-K., Yokoi K., 1984, ApJ, 286, 644
Nordström B., Mayor M., Anderson J., Holmberg J., Pont F., Jørgenson B.R., Olsen E.H., Udry S., Mowlavi N., 2004, A&A, 418, 989
Pancino E., Carrera R., Rossetti E., Gallart C., 2010, A&A, 511, 56
Proctor R.A., 1869, Proceedings of the Royal Society of London, 18, 169
Schiavon R.P., 2007, ApJS, 171, 146
Schlegel D.J., Finkbeiner D.P., Davis M., 1998, ApJ, 500, 525
Skuljan J., Hearnshaw J.B., Cottrell P.L., 1999, MNRAS, 308, 731
Takeda Y., Sato B., Murata D., 2008, PASJ, 60, 781
Wang L., Liu Y.J., Zhao G., Sato B., 2011, PASJ, 63, 1035
Woosley S.E., Weaver T.A., 1995, ApJS, 101, 181
Yi S.K., Kim Y.-C., Demarque P., 2003, ApJS, 144, 259
Yong D., Carney B.W., de Almeida M.L.T., 2005, AJ, 130, 597
Zhao J.K., Zhao G., Chen Y.Q., 2009, ApJ, 692, 113

SUPPLEMENTARY MATERIAL

The following supplementary material is available for this article online:

Table 6. All atomic-line data used for each sample star.

This paper has been typeset from a TeX/ LaTeX file prepared by the author.